Remote Sensing of Environment 112 (2008) 3594–3603

Contents lists available at ScienceDirect

Remote Sensing of Environment

journal homepage: www.elsevier.com/locate/rse

Fire-induced changes in green-up and leaf maturity of the Canadian boreal forest

Scott D. Peckham *, Douglas E. Ahl, Shawn P. Serbin, Stith T. Gower

Department of Forest and Wildlife Ecology, University of Wisconsin, 1630 Linden Drive, Madison, WI 53706, USA

ARTICLE INFO

Article history:
Received 25 July 2007
Received in revised form 12 March 2008
Accepted 30 April 2008

Keywords:
Leaf area index
Fire disturbance
Phenology
Modeling
Normalized difference vegetation index
Boreal forest
Canada

ABSTRACT

Recent studies of vegetation phenology of northern forests using satellite data suggest that the observed earlier spring increase and peak amplitude of the normalized difference vegetation index (NDVI) are a result of climate warming. In addition to undergoing an increase in temperature, the northern forests of Canada have also seen a dramatic increase in area burned by wildfire over the same time period. Using the Canadian Large Fire Database, we analyzed the impact fire had on the phenological dates derived from fitting a logistical model to yearly data from 2004 for several different subsets of both AVHRR-NDVI and MODIS LAI in wildfire dominated terrestrial ecozones. Fire had a significant but complex effect on estimated phenology dates. The most recently burned areas (1994–2003) had later green-up dates in two ecozones for AVHRR data and all ecozones for MODIS. However, older forested (not burned during 1980–2003) had estimated green-up dates 1 to 9 days earlier than the entire forested area in the MODIS LAI data. These data corroborate studies in Canada and demonstrate that fire history is influencing boreal forest phenology and growing season LAI.

1. Introduction

Forests in the boreal and high latitudes have experienced an increase in average temperatures over the past few decades (Solomon et al., 2007). This climate warming is expected to continue and current global circulation models predict increases of 2–4° C over the next 50 years (Solomon et al., 2007) for North America. Climate change affects the length of the growing season, photosynthetic activity, and carbon budget of the Canadian boreal forest. The earlier onset of the spring growing season has been observed in North America using temperature measures (Schwartz et al., 2006), lake ice break-up (Latifovic and Pouliot, 2007), and in the normalized difference vegetation index (NDVI) record (de Beurs and Henebry, 2005).

Recent studies have examined the phenology of vegetation in high northern latitudes, as expressed by changes in both NDVI data and net primary production (NPP) estimates using data from the polar-orbiting NOAA meteorological satellites. Some studies have concluded that spring green-up is occurring earlier (Myneni et al., 1997; Shabanov et al., 2002; Zhou et al., 2001) while others report an increase in magnitude (Tucker et al., 2001; Myneni et al., 1997; Slayback et al., 2003). The general conclusion from these studies is that vegetation in northern latitudes over the past 20 years is responding directly to increased temperature, with the effect of increasing the growing season and maximum leaf area index (LAI).

Wildfire is the most significant disturbance agent in the central Canadian boreal regions. Approximately three million hectares are burned annually in Canada alone (Kasischke and Stocks, 2000). This impacts forest age structure, as fires in the boreal region are typically large, intense, and stand replacing (Stocks, 1991). Young post-fire stands display a decrease in NDVI in the satellite record for several years following fire (Goetz et al., 2006). Because fire frequency and total area burned are increasing (Gillett et al., 2004; Stocks et al., 2003), it is important to differentiate the effect of wildfire versus climate warming on start of growing season and leaf maturity. In other words, since fire directly affects species distribution in boreal regions, we are investigating the relationship between fire, tree species distribution, and pixel level phenology. Wildfire disturbance also affects carbon dynamics of forests in the northern hemisphere, especially in the boreal zone (Bond-Lamberty et al., 2004; Kasischke and Stocks, 2000; Wang et al., 2003; Bond-Lamberty et al., 2007). Understanding the role fire disturbance plays in the signal measured by satellite sensors could aid and improve modeling the effects of climate, CO_2, fire, and their interactions on vegetation phenology and NPP estimates.

The two objectives of this study were to (1) determine onset of spring and leaf maturity dates for terrestrial ecozones of Canada based on time since fire and (2) assess the impact forest fire has on estimated dates for study area on an ecozone basis.

Both the fire regime and vegetation phenology in the study area are undoubtedly linked to climactic factors (Johnson, 1992; Chen et al., 1999). Temperature and precipitation can influence both the start of the growing season (Lucht et al., 2002; Chen et al., 1999) and the

* Corresponding author. Tel.: +1 608 265 5628; fax: +1 608 262 9922.
E-mail address: sdpeckha@wisc.edu (S.D. Peckham).

0034-4257/$ – see front matter © 2008 Elsevier Inc. All rights reserved.
doi:10.1016/j.rse.2008.04.016

distribution and area burned by wildfire (Johnson, 1992). This influence can vary in both time and spatial extent. In order to separate climactic influence from geographic position, data was analyzed using the 15 terrestrial ecozones of Canada (Ecological Stratification Working Group, 1996). The ecozone is the top level of generalization of the land surface area of Canada. We analyzed one growing season and the response of burned versus non-burned pixels for those ecozones with large enough sample of burned pixels. Using AVHRR and MODIS data from 2004, seven data subsets were extracted and analyzed by fitting a logistic model. This approach is desirable because it has model parameters that describe vegetation phenology for both a temperate deciduous forest (Ahl et al., 2006) and a high latitude boreal forest (Beck et al., 2006).

This study is relevant as global circulation models are predicting continued warming and increased CO_2 levels in northern latitudes with subsequent lengthening of the growing season, decrease in permafrost, and increase in photosynthetic activity of vegetation in northern latitudes. In addition, area burned by wildfire has increased significantly in the past decades (Stocks et al., 2003) and it is critical to understand how the Canadian forest biome is responding to these climatic and disturbance factors as measured by remote sensing, and how to reliably estimate and quantify the changes in forest phenology, whether due to climate or fire disturbance.

2. Methods

2.1. Study area

This study focused on the boreal and transitional forested area of Canada (Fig. 1). It comprises 75–77% of Canada's forested area (Natural Resources Canada, 2006a; Kurz and Apps, 1999) and has been the focus of numerous terrestrial carbon cycle studies. We concentrated on four of the 15 terrestrial ecozones (Fig. 2) — the Taiga Plains (TP), Taiga Shield (TS), Boreal Shield (BS), and Boreal Plains (BP) because 96% of the burned area locations extracted for this study occurred in these ecozones. Located primarily in the western portion of the Northwest Territories and northern British Columbia and Alberta, the Taiga Plains ecozone is the northern edge of the boreal coniferous forest, an open canopy black spruce (*Picea mariana*) dominated landscape with well-developed shrub and understory layers. Shrub species include dwarf birch (*Betula nana*), Labrador tea (*Ledum groenlandicum*), and willow (*Salix* spp.). Understory species include bearberry (*Arctostaphylos uva ursi*), mosses, and sedges. Mean annual temperatures range from −10 to −1° C, and mean annual precipitation ranges from 200–500 mm. To the east of the Taiga Plain lies the Taiga Shield. This ecozone is divided by Hudson Bay with mean annual temperatures around −8° C in the west and 0° C in the east. Precipitation ranges from 200–500 mm in the west and 500–800 mm east of Hudson Bay. Forests become more open and shorter stature with increasing latitude. Black spruce and jack pine (*Pinus banksiana*) occur throughout, with tamarack (*Larix laricina*), alder (*Alnus crispa*), and willow in wetlands. Trembling aspen (*Populus tremuloides*) and balsam poplar (*Populus balasmifera*) are found in upland areas. The Boreal Shield is the largest of the Canadian ecozones. It stretches from northern Saskatchewan to Newfoundland. Mean annual temperature ranges from −4 to 5.5° C, and rainfall 400 to 1000 mm, in the western and eastern regions, respectively. The forest is predominantly closed and comprised of black and white spruce, balsam fir, and tamarack. Trembling aspen, balsam poplar, and white birch are found in the southern regions. The final ecozone used in this study, the Boreal Plain, is situated to the south of the Taiga Plain and east of the Boreal Shield. Mean annual temperatures average −2 to 2° C and precipitation 300 to 625 mm. Black spruce and tamarack dominate in the northern regions, while trembling aspen, and balsam poplar are more common in the southern.

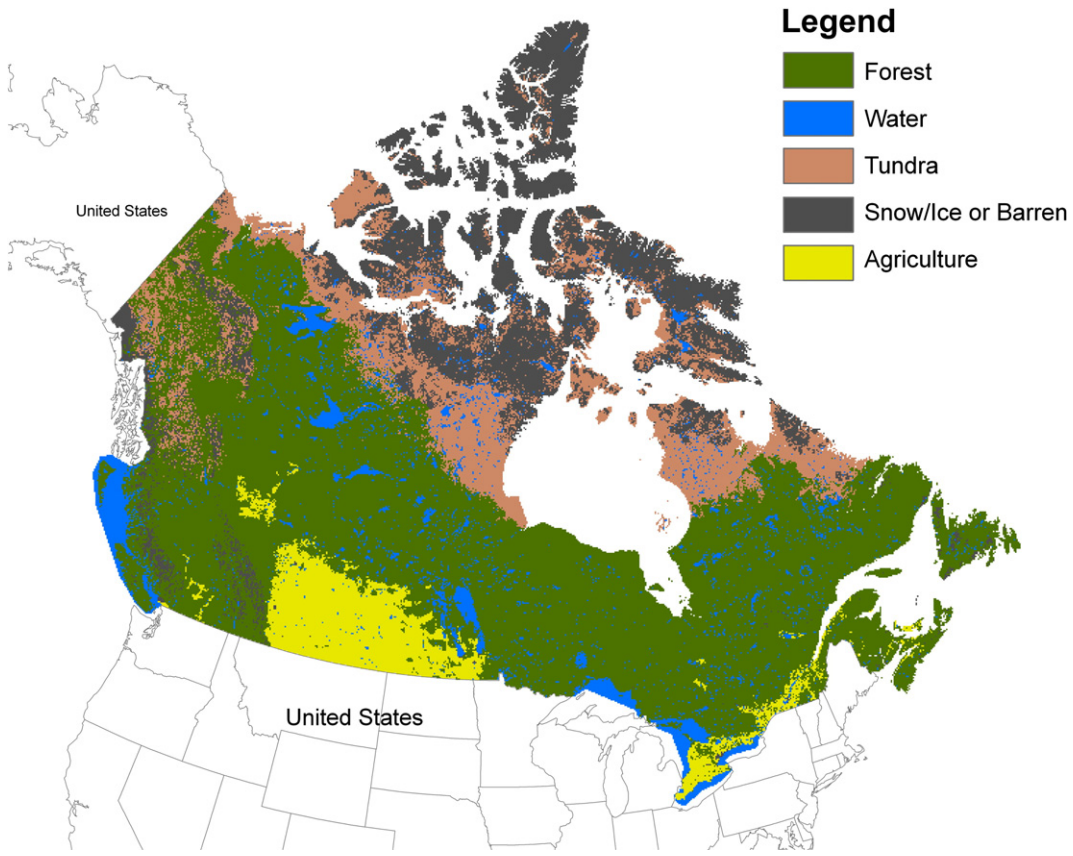

Fig. 1. Land cover of Canada used in this study. The dark green region corresponds to the forested area used to subset the AVHRR and MODIS data.

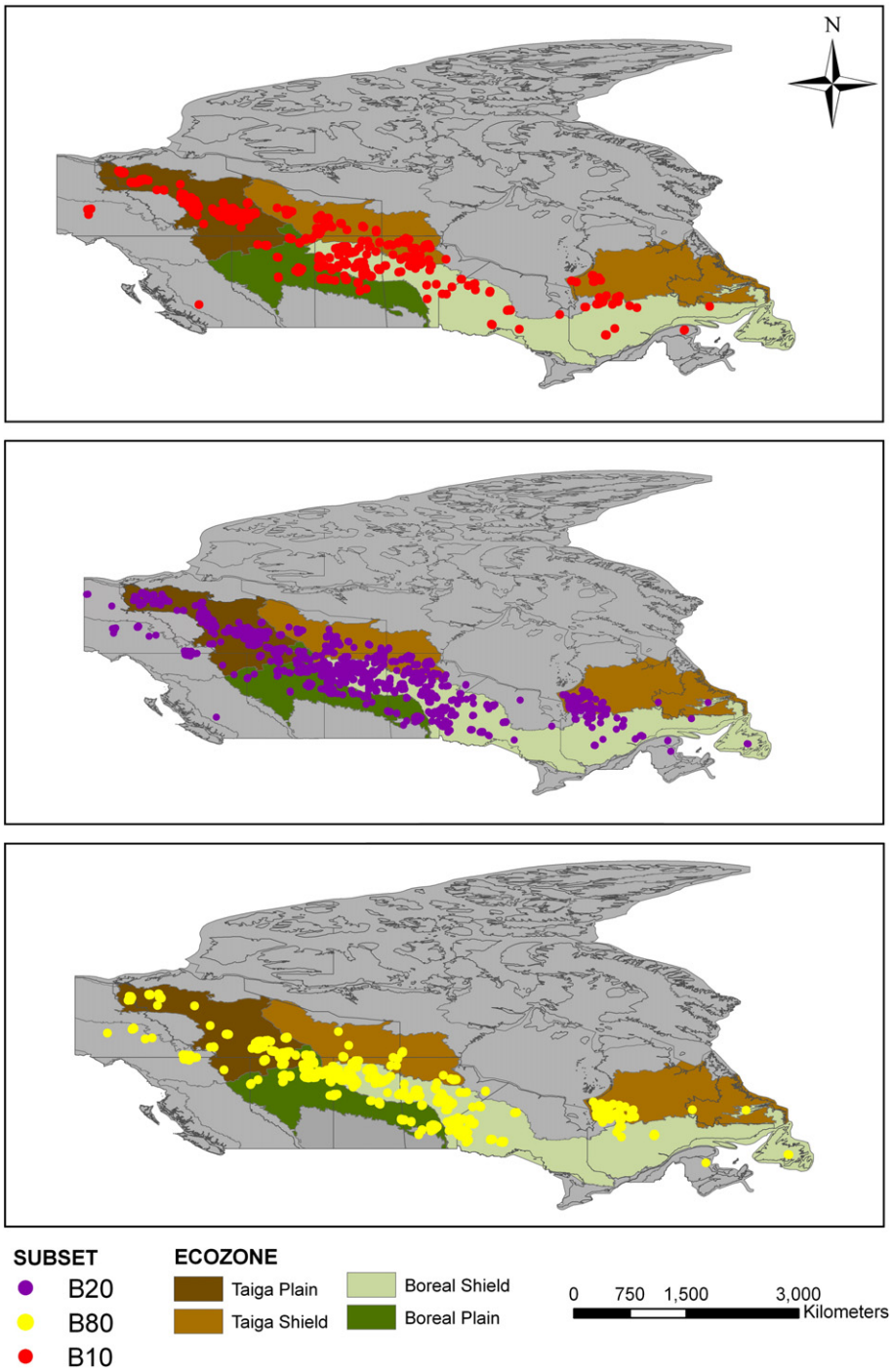

Fig. 2. Maps of the three different burn subsets. Locations of pixels extracted from satellite imagery are show with colored circles. Canadian province boundaries outlines are overlaid on the Canadian terrestrial ecozones. Ecozones used in this study are shown in color other than gray.

For both AVHRR and MODIS, seven different data subsets were created and analyzed (Table 1) before data was narrowed down to the four ecozones described above. The data set consisted of the entire forested area of Canada, as indicated by the land cover classification of Canada (Fig. 1), denoted "AF". We selected a subset that included burns that occurred during 1994–2003 (B10). This first subset was chosen to represent recently burned areas as Goetz et al. (2006) found that it took approximately 10 years for NDVI to recover to pre-burn levels following fire. In addition, a subset of all forested areas without these burns was also created (NB10). All years of burns available (1980–2003) in the CLFD spatial data set (B20) and the non-burned forested (NB20) were analyzed. Finally, we examined the impact of the large burn years that occurred during the 1980s creating two more subsets with and without burns that occurred between 1980 and 1989 (B80 and NB80). The burned subsets are mapped in Fig. 2.

2.2. Spatial data

Several data sets from varying sources were obtained for this study. The Canadian land cover data set (Palko et al., 1993; Natural Resources Canada, 2006b), derived from AVHRR data, was reprojected to match the GIMMS NDVI Albers equal area conic projection, and resampled to 8 km resolution using nearest neighbor interpolation. It was then used as a masking layer to select desired regions from the NDVI imagery

Table 1
Data subsets created for this study

Data subset	Description	Number of pixels extracted
AF	The *x,y* location of all GIMMS pixels identified as forested in the land cover map	84,744
B10	Pixels that were both forested and completely burned during 1994–2003	688
B20	Pixels that were both forested and completely burned during 1984–2003	1671
B80	Pixels that were both forested and completely burned during 1980–1989	875
NB10	Forested pixels not burned during 1994–2003	84,073
NB20	Forested pixels not burned during 1984–2003	61,170
NB80	Forested pixels not burned during 1980–1989	83,882

Locations were based on the coordinates of selected GIMMS pixels. The third column shows the number of AVHRR pixels extracted from each image for each data subset prior to quality flag screening.

(forest versus non-forest). We retained all classified forest types in this analysis. Of these forested areas, 5.6% were broadleaf, 20.4% mixed, 25.6% transitional, and 48.4% were coniferous, based on the Canadian vegetation classification system (Strong et al., 1990).

We used an updated version of the Canadian Large Fire Database (CLFD) (Stocks et al., 2003) containing polygon coverage of burn area for years 1981–2003 (Canadian Forest Service). This GIS data set consists of digitized and geo-referenced fire data from Canadian agencies and includes all fires greater than 200 ha in size. The fire data set was reprojected to match the NDVI and land cover data and used to isolate pixels burned during specific years. We then used these locations to extract pixel values from the NDVI and LAI time series data.

An index grid of the same spatial extent and resolution of the NDVI data set was created and joined with the CLFD using ArcGIS (ESRI, 2006). Each grid index pixel then contained the area burned in a specific year, and it was possible to have more than one burn year in a given pixel. This method was chosen to retain as much information as possible, although in this study only pixels that were completely burned in a single year (i.e. burn year area was 64 km^2) were used to minimize variability and avoid mixed pixel effects. A lookup table was built that contained locations of all pixels to extract from the NDVI data. The number of pixels extracted for each data subset is shown in Table 1. We also identified a set of 'unburned' locations to complement each 'burned' data subset. These were pixels that were both forested and had not been burned at all during the years in the complementary 'burned' period (i.e. 1994–2003). In this study, we denote these as 'unburned' pixels. We acknowledge the possibility that some of these areas could have burned relatively close to the earliest year available in the CLFD data set. All of the burned data subsets are mapped in Fig. 2.

We modeled NDVI phenology using the GIMMS NDVI-G data set for North America (Brown et al., 2004; Tucker et al., 2005). Images obtained from the Goddard Space Flight Center and covering North America in 2004, were subset to include the Canadian provinces. Using the fire data described above, NDVI data were extracted for each major burn year by using only pixels that fell completely within a given burn polygon (Table 1) and then restricted to flag values of zero (good data). This procedure was applied to all available NDVI images from 2004. All image processing was done using IDL (ITT, 2006) and output was written to a file for input into SAS (SAS Institute, 2006).

LAI phenology was modeled using collection four (V004) of the MOD15A2 MODIS/Terra Leaf Area Index/FPAR 8-day L4 product. All available data sets for 2004 from ten tiles (Table 2) were used to cover the majority of the Canadian boreal forest. A sample of pixels from each image was extracted using programs written in IDL and ENVI (ITT, 2006) and saved to a file for input to SAS. Extracted MODIS pixels were determined by using the latitude and longitude of each AVHRR pixel used in the analysis described above. Data were filtered using the quality control (QC) fields, restricting data to cloud-free, and generated using the main radiative transfer (RT) model.

We computed the normalized difference water index (NDWI) (Gao, 1996), using the MOD09 surface reflectance product (Vermote et al., 1997), to compare the NDVI and MODIS time series to snowmelt. The same tiles were obtained as above and values were computed at the same spatial locations in the study area to investigate the estimated start of season dates derived from NDVI and LAI and their relationship to the beginning of snowmelt and start of season as indicated by NDWI. Inference on beginning of snowmelt and start of growing season follow methods described by Delbart et al. (2005). Pixels extracted from all remote sensing data were assigned an ecozone value. A polygon coverage of the Canadian terrestrial ecozones (http://www.agr.gc.ca/nlwis/index_e.cfms=data_donnees&s=details&page=eco_plus) was used to determine the appropriate ecozone for each pixel extracted from the imagery.

2.3. Statistical analysis and phenology extraction

The first step in our analysis was to examine the time series of each data subset in each ecozone. Mean values at the time point nearest the middle of July for all data sets were compared using one-way ANOVA and contrasts were made using the 'multcomp' package in R (R core development team, 2006). We chose the second composite image in July for AVHRR and day 193 for MODIS LAI. These dates were selected because they correspond to the maximum mean LAI value for boreal forests (Serbin et al., submitted for publication; Chen, 1996; Pisek & Chen, 2007). Significance was assessed at the 0.05 level in all tests.

Start of season, or green-up, and maturity dates for both MODIS LAI and AVHRR-NDVI were determined by fitting a logistic model to the seasonal data using methods outlined in Ahl et al. (2006). These dates were determined by computing local maxima of the derivative of the curvature function of the logistic model. Monte Carlo simulation using the MODEL procedure in SAS with twenty thousand permutations was used to determine average growing season start and maturity dates for each data set as well as 95% confidence intervals.

2.4. Plantwatch observations

A volunteer phenology network, such as plantwatch, is a potential source of validation for phenology estimates derived from remote sensing. All plantwatch data were obtained (http://www.frogwatch.ca/english/plantwatch/) and reduced to observations for aspen from 2004. Results were then mapped to determine an ecozone for each observation. Average dates of appearance for aspen were determined for two of the four ecozones (BP and BS). A large portion of this study area lies in regions of Canada with few or no roads, so it is understandable that well-distributed field data are not available for all

Table 2
MOD15A2 data summary for B20 and NB20

Tile	Number of images	Burned pixels extracted per image	Non-burned pixels extracted per image
h10v03	46	1	6336
h11v02	46	13	1955
h11v03	46	200	8535
h12v02	46	479	5688
h12v03	46	545	8757
h13v02	46	5	2796
h13v03	46	199	6748
h14v03	46	3	5329

The table illustrates number of pixels extracted from the 8 tiles used to cover the study area.

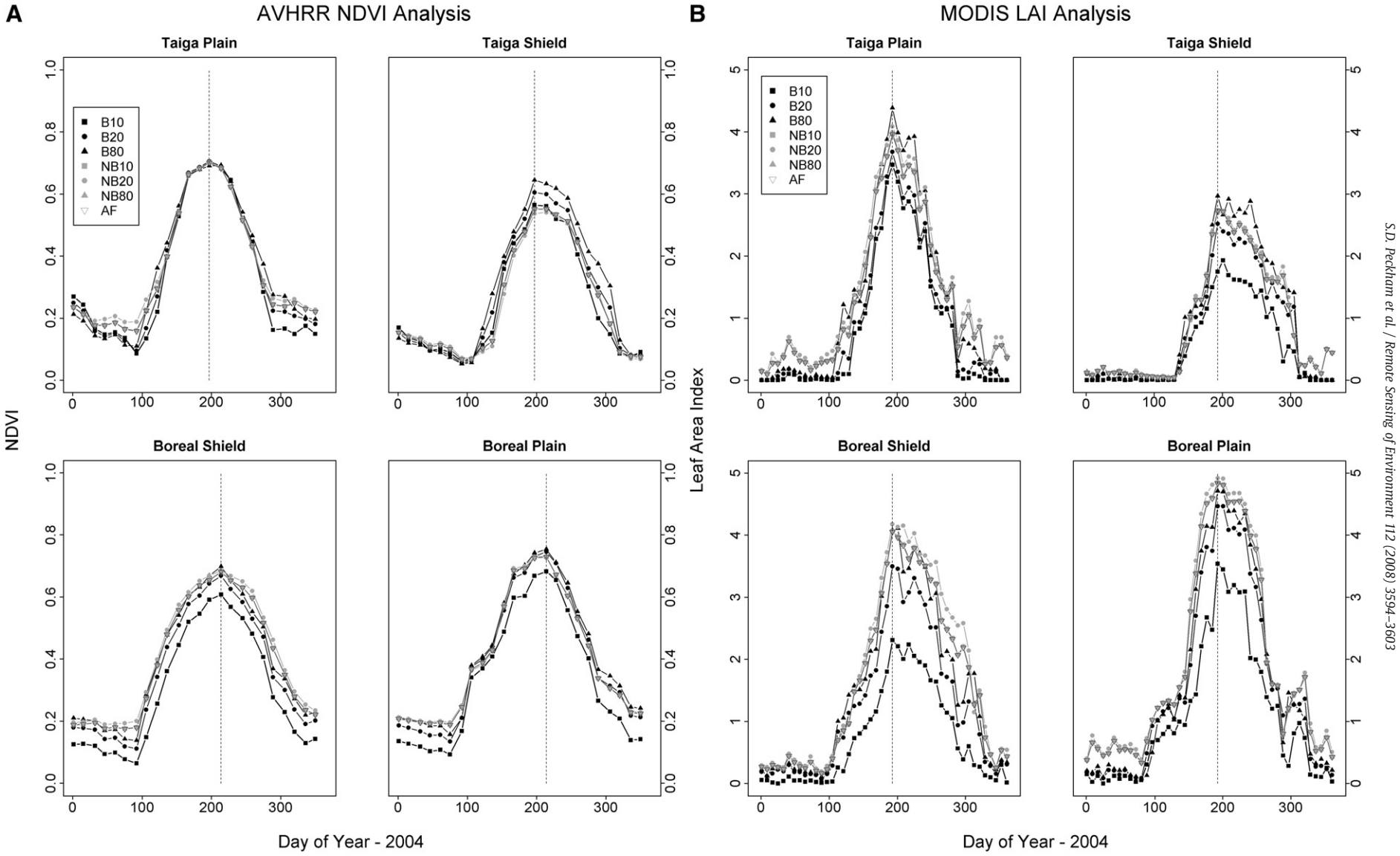

Fig. 3. Year 2004 time series plots for A) AVHRR-NDVI, B) MODIS LAI, and C) MODIS NDWI. For the AVHRR time series, the first monthly composite is plotted on the first of the month and the second on the 15th of the respective month. For MODIS, data is plotted corresponding to the number of each 8-day composite. The vertical dashed line denotes where the one-way ANOVA and contrasts of mean values were performed.

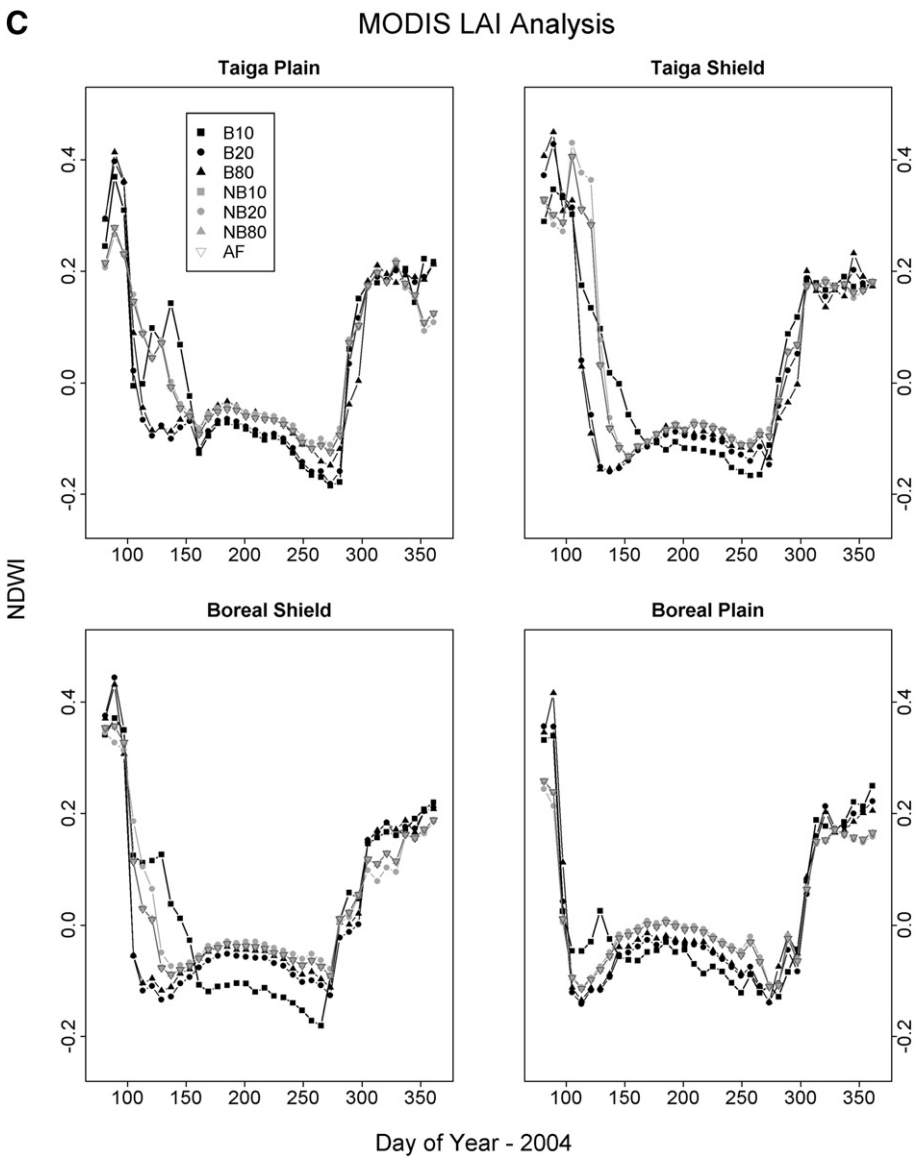

Fig. 3. (*continued*).

ecozones. We present the data for comparison purposes as it presents an opportunity for future study.

3. Results

3.1. Time series analysis

Plots of the seven NDVI data subsets for each ecozone are shown in Fig. 3a. Within each ecozone, the time series are quite similar to one another. Observed maximum NDVI values for all subsets occurred during the same NDVI composite except for B10 in ecozone 4, which had a maximum in the first composite period in August. Results of the multiple contrasts are shown in Fig. 4a. All data subsets were contrasted against AF, but we were most interested in NB10 (forest without most recent burns), NB20 (forest without all burned pixels), and NB80 (forest without burns from 1980s) contrasted with AF (entire forested area). Some of these contrasts were significant ($p<0.05$), suggesting that in some ecozones the burns that occurred since 1980 are influencing maximum NDVI, since removing burned areas significantly affected this value. In two ecozones, the recently burned (B10) areas have a lower value than NB10 and AF (0–53%). B80 had the largest maximum NDVI values and were significantly different from the 'unburned' data in two ecozones (TS and BP) (Fig. 4a). Results from this study indicate that the most recently burned areas in the boreal ecozones tended to be lower in magnitude in almost every NDVI compositing period, but recover 15–20 years later to values higher than stands of older age.

The plots of the seven LAI data sets for each ecozone are shown in Fig. 3b. Similar to NDVI, the time series within each ecozone share similar trajectories. It is interesting to note that B10 was significantly lower in maximum LAI ($p<0.001$) when compared to the entire forested area (AF) in all four ecozones (Fig. 4b). We anticipated that the unburned, older age forest would exhibit a higher maximum LAI than younger stands, and this was observed in the MODIS signal. The contrast between NB20 and AF was significant ($p<0.05$) in the TP, BS, and BP ecozones. In all cases NB20 is larger than AF, suggesting that 20 years of fires in these ecozones decreased observed LAI.

The unburned signal in all ecozones does not seem to be dominated by conifer forest, as it would be expected to show less seasonality than in Fig. 3b. Serbin et al. (submitted for publication) showed that overstory LAI of black spruce forest stands greater than 70 years of age did not vary seasonally. The overstory LAI of a coniferous forest should not change as dramatically as the signal in Fig. 3, suggesting that the signal is being driven by other vegetation —

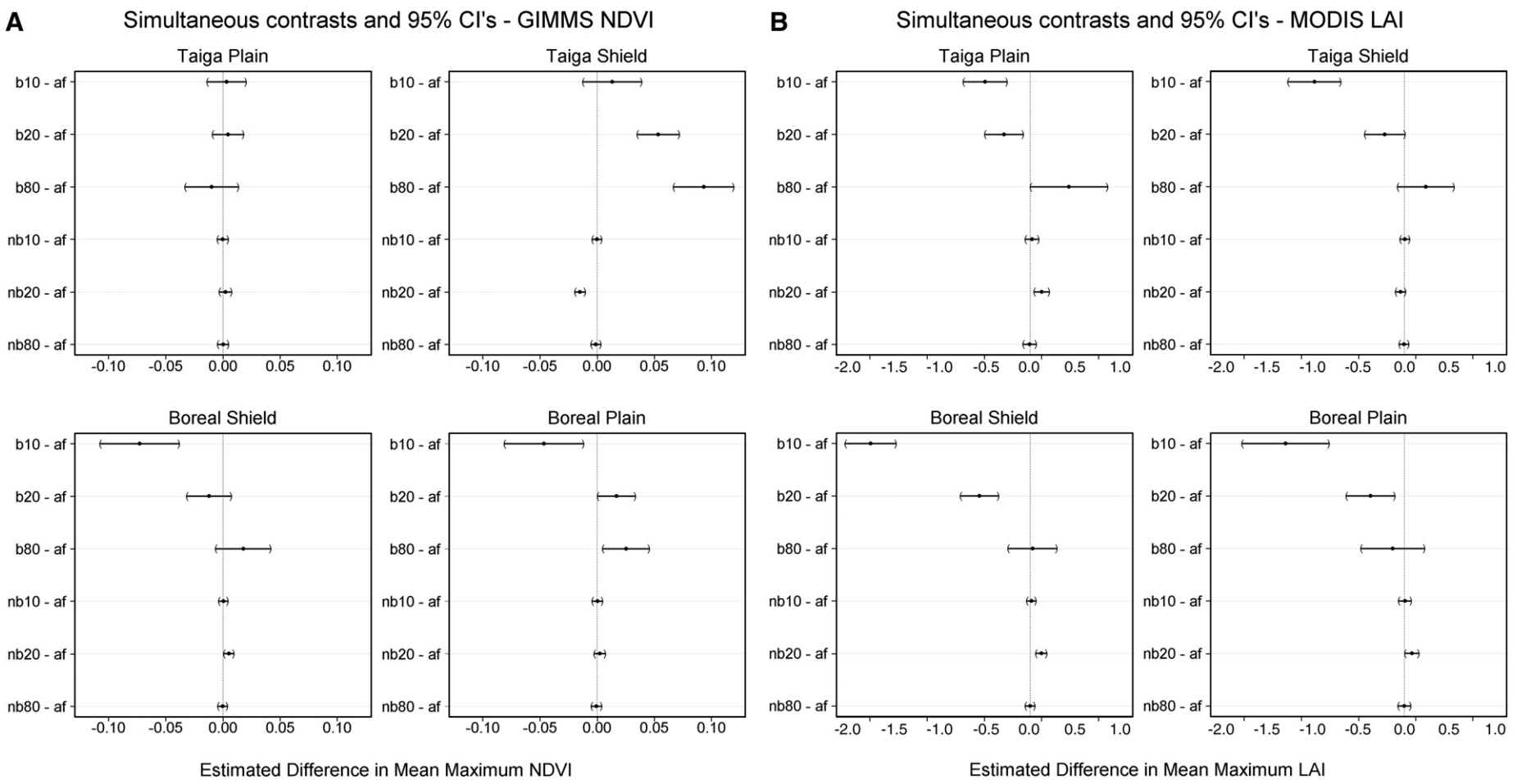

Fig. 4. Multiple simultaneous contrasts of the seven data sets for A) AVHRR-NDVI and B) MODIS LAI. The estimated difference in mean value (at day of year corresponding to dashed vertical line in Fig. 3) is plotted along with the associated 95% confidence interval. Intervals that do not include 0.0 are considered significant at the 0.05 level.

Table 3
Model estimated spring phenology dates for NDVI (a) and LAI (b)

a)

Subset	Taiga Plain (116)	Taiga Shield (137)	Boreal Shield (98)	Boreal Plain (90)
B10	6	−4	8	−15
B20	0	−13	2	−8
B80	−12	−21	0	−1
NB10	0	0	0	0
NB20	−1	3	−2	3
NB80	1	0	0	0

b)

Subset	Taiga Plain (142)	Taiga Shield (159)	Boreal Shield (139)	Boreal Plain (138)
B10	8	12	23	12
B20	9	14	20	5
B80	7	15	19	2
NB10	−1	0	0	0
NB20	−4	−7	−9	−1
NB80	0	−1	0	0

Days are given relative to the estimate for AF in each ecozone, which are shown in parentheses.

deciduous over- and understory. The conifer overstory contribution seems to stand out in the time outside of the growing season as the unburned forest LAI is on average 13 times larger (1100%) during these time periods.

3.2. Phenology detection

Model estimated green-up and maturity dates for GIMMS NDVI are shown in Tables 3a and 4a, respectively. B80 had the earliest estimates (day 104 and 116) in ecozones 4 and 5. When compared to their 'unburned' counterparts, these dates are on the order of, or greater than the 15-day compositing resolution of the data. Unburned subsets NB10, NB20, and NB80 estimates along with AF were within 3 days of one another in all four ecozones. Removing the burned locations from the NDVI data did not change the start of season estimate greater than 15 days (temporal resolution of the data). Estimates for the peak of the growing season varied among ecozones, but within ecozone variation was low (2–5%). In ecozone 5, B80 had an estimated peak at day 196. This falls in the composite covering the second half of July, while all other estimates of peak growing season in this ecozone fall in the previous NDVI composite. In ecozone 9, both B10 and B20 had estimates in the second half of July (day 197) compared to the rest of the data subsets in the first half of July.

Table 4
Model estimated leaf maximum dates for NDVI (a) and LAI (b)

a)

Subset	Taiga Plain (177)	Taiga Shield (188)	Boreal Shield (173)	Boreal Plain (194)
B10	−5	−4	6	3
B20	−4	2	3	3
B80	−4	8	2	−1
NB10	0	0	0	0
NB20	2	2	0	−1
NB80	0	0	0	0

b)

Subset	Taiga Plain (176)	Taiga Shield 189)	Boreal Shield (192)	Boreal Plain (171)
B10	5	1	−1	17
B20	4	−1	−5	9
B80	2	−2	−7	6
NB10	0	0	0	0
NB20	−2	1	2	−2
NB80	0	0	0	0

Days are given relative to the estimate for AF in each ecozone, which are shown in parentheses.

Table 5
Start of season estimates derived from the NDWI time series (Fig. 3c)

Subset	Taiga Plain (169)	Taiga Shield 161)	Boreal Shield (145)	Boreal Plain (121)
B10	0	–	32	–
B20	0	−16	−8	0
B80	0	−16	−8	0
NB10	0	0	0	0
NB20	0	0	0	0
NB80	0	0	0	0

Days shown are relative to the estimate for AF (shown in parentheses next to the ecozone).

The LAI of burned areas (B10, B20, B80) had green-up dates much later than their 'unburned' counter parts (NB10, NB20, NB80), as well as the entire forested area (Table 3b) for all four ecozones. NB10 and AF were not significantly different from one another (their 95% confidence intervals do not overlap). With this level of sampling from the MODIS imagery, removing locations burned within the last 10 years did not have an effect on the estimate of start of season. In all ecozones except 9, all burn data sets' estimates fall at least one 8-day period later than NB10, NB20, NB80, and AF. However for NB20, the start of season estimate was significantly earlier ($p<0.05$), than AF, when all burned pixels were removed. Although all were statistically significant ($p<0.05$), only the estimate in BS ecozone was in a different 8-day composite image period.

Estimated dates of maximum LAI for B10, B20, and B80 were one 8-day composite later than NB10, NB20, NB80, and AF in both ecozone 4 and 9 (Table 4b). In the other two ecozones, all estimates of maximum LAI fell in the same image composite. Maximum LAI for NB10, NB20, and NB80 did not differ significantly from AF (confidence intervals all overlap). This suggests that on average, both burned and unburned forests are reaching peak LAI during the same 8-day period image composite period in the TS and BS ecozones. In the TP and BP ecozones, NB20 was significantly different than NB10, NB80, and AF, but the estimates only differed by about 2 days. For both ecozones the estimates were earlier than the rest of the unburned and forested subsets.

NDWI has also been used to determine phenological dates (Delbart et al., 2005, 2006). NDWI decreases in spring, indicating the beginning of snowmelt and then increases with emergence of leaves (Delbart et al., 2005). To compare with snowmelt, we computed the NDWI for each data subset in each ecozone (Fig. 3c). Both NDVI and LAI increased during the period NDWI decreased — indicating that both average NDVI and LAI begin to increase during snowmelt. Table 5 shows the 8-day composite in which green-up is estimated using NDWI. Both TP and BP ecozones did not show a difference between burned and unburned data. In TS and BS ecozones, B20 and B80 had green-up dates that were one 8-day composite period earlier than their unburned counterparts. We were unable to derive a green-up estimate for B10 of TS and BP ecozones because the pattern following snowmelt did not exactly follow the pattern of greening vegetation as observed by Delbart et al. (2005), it just continued to decrease throughout the growing season. This high degree of variability could be due to these recently burned area's lack of vegetation in some cases. This contradicts the LAI time series observed for these data subsets in Fig. 3b. More detailed investigation is needed to completely understand this result.

3.3. Comparison with plantwatch

Although observations in the plantwatch network were very limited in the study area, we felt that the data may provide a meaningful comparison to phenology dates derived from remote sensing. Average estimates of aspen leaf appearance for BS and BP ecozones were days 142 and 132, with a total of ten and three

observations, respectively. We compared the plantwatch observations to all estimates from remote sensing by computing the average difference between plantwatch and each remote sensing subset for each ecozone. In BS ecozone, both NDWI and LAI estimates were about 5 days later than plantwatch. In BP ecozone, the NDWI estimate was 11 days earlier than plantwatch, while the average LAI estimate was 8 days later. The average difference between the NDVI estimate and plantwatch was 43 and 45 days earlier for BS and BP ecozones, respectively. Clearly, in these regions LAI and NDWI estimates were more correlated to aspen green-up than NDVI. This was an interesting and unexpected result.

4. Discussion

Maximum NDVI for B10 was lower than NB10 and AF in two ecozones. This result is supported by Goetz et al. (2006), who found that NDVI anomalies tended to be lower following fire, and took 5–10 years to recover to pre-burned levels. Time series results, which showed that most recently burned areas tended to be lower in magnitude in every NDVI compositing period but recover 15–20 years later to values higher than stands of an older age, are consistent with direct and optical field measurements for a wildfire chronosequence in Manitoba Canada (Bond-Lamberty et al., 2002; Serbin et al., submitted for publication). In the LAI time series data, B10 was significantly lower than NB10 and AF in all ecozones. Our results are consistent with Bond-Lamberty et al. (2002) who found that young burned stands are dominated by shrubs and regenerating deciduous species with LAI of approximately 1–3, and LAI is at a maximum of about 70 years following fire in boreal black spruce.

Green-up estimates from GIMMS NDVI were much earlier than those derived from MODIS LAI, MODIS NDWI, and plantwatch. NDVI is a reasonable surrogate for photosynthetic activity (Tucker, 1979), but it appears that NDVI increase in spring in high latitude biomes may be correlated to snowmelt (Fig. 3a and c; Moulin et al., 1997). Our results support this conclusion. Detailed phenology measurements at a boreal forest wildfire chronosequence (Serbin et al., submitted for publication) observed green-up at all sites in 2004–2006 were later than day 130. These dates are more than 30 days later than those derived from GIMMS NDVI for the BS ecozone (Table 4a). Our hypothesis cannot be confirmed without a well-distributed set of field measurements covering this vast study area, but observed results in this study are likely due to a combination of reduction in snow cover revealing existing understory (mosses, lichens, etc.). In addition, GIMMS NDVI has a relatively poor temporal and spatial resolution compared to MODIS.

Photosynthetic activity and plant growth in older stands with well-developed canopy and existing woody and non-herbaceous understory and ground cover are detected earlier by MODIS LAI than young, recently burned stands. In all ecozones, green-up occurred by as much as 30 days later in recently burned than unburned areas (Table 3b). The exact reason for this is unclear, but it may be related to forest stand composition. In the northern Manitoba region, post-fire stands of less than 10 years have low LAI (<2.0) and are dominated by shrubs and other herbaceous cover (Bond-Lamberty et al., 2002; Serbin et al., submitted for publication). Our results corroborate those of Serbin et al. (submitted for publication) who found that green-up occurred 7–10 days earlier in the 15–30-year old stands than in stands of 0–15 years. The 15–30-year old stands have large component of aspen while the younger stands (0–15) are comprised of shrubs, grasses, sedges and herbs. It appears that the presence of aspen in the over- or understory is the cause of the earlier green-up observed in the field and with remote sensing. Barr et al. (2004) found that aspen green-up occurred earlier than hazelnut, another deciduous species. In this study, B80 (15–24-year old stands) had an earlier start of season estimate when compared to B10 (1–10-year old stands) in 3 of 4 ecozones.

Table 6
MODIS MOD12Q1 land cover type 3 percentages for the three burned and one unburned data subsets

Type 3 land cover	B10	B20	B80	NB20
Water	0.19	0.17	0.44	0.74
Grasses/cereal crops	2.42	2.44	0.44	1.74
Shrubs	86.78	67.94	50.66	38.18
Broadleaf crops	0.00	0.00	0.00	0.21
Savannah	0.00	1.39	3.06	3.16
Broadleaf forest	0.00	0.00	0.00	0.43
Needleleaf forest	8.94	28.05	45.41	55.30
Unvegetated	1.68	0.00	0.00	0.22
Urban	0.00	0.00	0.00	0.01

It is possible that other factors could also influence the observed effect fire had on phenology in this study. One example is the land cover classification used to drive the LAI algorithm. If the MOD12Q1 land cover product incorrectly classified pixels in the study area, LAI values, and hence phenology estimates could potentially be incorrect. Table 6 shows land cover type 3 percentages for each of the different burn subsets. This analysis suggests that on a regional basis the algorithm is appropriately classifying burned pixels (within the classification scheme), as burned stands are replaced by shrubs and young deciduous tree species. The younger stands are predominantly classified as shrubs (87%) with very few needleleaf pixels (9%). This changed to needleleaf dominant as the stand age increased (i.e. NB20, Table 6). The land cover classification scheme used in the MOD15 product does not provide for a mixed deciduous/coniferous forest. Perhaps the release of version 5 of the LAI product and improvements in land cover classification will result in even better estimates of phenology from MODIS. Another possible impact to results observed in LAI and NDWI was the sampling used. Locations processed from MODIS data used the same coordinates as pixels extracted from GIMMS NDVI. Data sets like B10, which had the smallest number of pixels could potentially contribute more to the overall signal if the resolution of the MODIS data was fully utilized. A more intense sampling of pixels on a smaller spatial scale (i.e. ecoregion) could provide even more information on how fire influences the phenology of the boreal landscape that seems warranted.

Although both LAI and NDWI are relatively close when compared to dates from plantwatch, the effects of wildfire on estimating phenology were different between them. While burned area start of season estimates in MODIS LAI were consistently later than their unburned counterparts across ecozones, NDWI estimates were not. In fact, the opposite was observed in NDWI. In two ecozones (5 and 6) B20 and B80 estimates were 16 and 8 days earlier than unburned regions. Burned area LAI estimates were 2–23 days later than unburned areas. Whether this is due to purely to the vegetation response and recovery after fire, regional climactic or hydrologic conditions in 2004, or a combination of these is beyond the scope of this analysis, but deserves further study.

The estimates of peak LAI varied by ecozone and time since fire, but effects of the burned areas were less pronounced than green-up estimates. NDVI and LAI estimates generally agreed (<10 days) in TP and TS ecozones, but differed by up to 24 days in BS and BP ecozones. This again stresses the importance of accounting for regional variation in vegetation monitoring using remote sensing data.

5. Conclusions

This study investigated the effect of fire on phenology using several remotely sensed data sources. While both regional temperature and precipitation may be the primary drivers of phenology at a specific locale, we assessed the phenology of pixels based on time since fire within each ecozone. Significant increases in temperature and fire in the Canadian boreal zone could result in a shift in stand age as a result

of wildfire, and hence phenological change at regional or even continental scales.

There were two key findings in this study. First, our results suggest that wildfire activity during 1994–2003 in the Canadian boreal forest did not affect green-up estimated from AVHRR-NDVI and MODIS LAI products in 2004 at the level of sampling used in this study. Although start of season dates in B10 were significantly later than unburned and AF in all ecozones, estimates for NB10 did not differ significantly from AF. Second, our findings indicate that burns that occurred during 1980–2003 have a significant impact on model estimates of green-up and maximum LAI estimates derived from MODIS. NB20 had estimates that were both significantly earlier than AF in three of the four ecozones analyzed. In addition, significant decreases, driven by this subset, were observed in maximum LAI.

Although the phenology dates differed among the different remote sensor data and ecozones, our results indicate that fire influences phenology dates derived from satellite data. The effects burned areas have on green-up and maximum LAI as well as regional effects on ecosystem response following fire should be considered in NPP estimates. Interannual variation in these estimates should also be investigated to determine if regional results obtained in this study are consistent from year to year. Differentiating burned areas and time since fire could improve global estimates of terrestrial NPP — especially with methods using satellite-derived NDVI. More research is needed to estimate the impacts incorporating stand age relationships and the contribution of bryophytes to phenology estimates and global carbon balance estimates made using products developed from remotely sensed data.

Acknowledgements

This research was supported by NASA grant NNG04GL26G to S.T. Gower and D.E. Ahl. We thank Molly Brown at the NASA Goddard Space Flight Center for access to the 2004 GIMMS NDVI data and Mike Flannigan at the Canadian Forest Service for the updated fire polygon data. The authors also thank the three anonymous reviewers whose comments greatly improved the manuscript.

References

Ahl, D. E., Gower, S. T., Burrows, S. N., Shabanov, N. V., Myneni, R. B., & Knyazikhin, Y. (2006). Monitoring spring canopy phenology of a deciduous broadleaf forest using MODIS. *Remote Sensing of Environment*, *104*, 88–95.

Barr, A. G., et al. (2004). Inter-annual variability in the leaf area index of a boreal aspen-hazelnut forest in relation to net ecosystem production. *Agricultural and Forest Meteorology*, *126*(3–4), 237–255.

Beck, P. S. A., Atzberger, C., Hogda, K. A., Johansen, B., & Skidmore, A. K. (2006). Improved monitoring of vegetation dynamics at very high latitudes: A new method using MODIS NDVI. *Remote Sensing of Environment*, *100*(3), 321–334.

Bond-Lamberty, B., Peckham, S. D., Ahl, D. E., & Gower, S. T. (2007). Fire as the dominant driver of central Canadian boreal forest carbon balance. *Nature*, *450*, 89–93.

Bond-Lamberty, B., Wang, C., & Gower, S. T. (2004). Net primary production and net ecosystem production of a boreal black spruce wildfire chronosequence. *Global Change Biology*, *10*, 473–487.

Bond-Lamberty, B., Wang, C., Gower, S. T., & Norman, J. (2002). Leaf area dynamics of a boreal black spruce chronosequence. *Tree Physiology*, *22*, 993–1001.

Brown, M. E., Pinzon, J. E., & Tucker, C. J. (2004). New vegetation index data set to monitor global change. *American Geophysical Union EOS Transactions*, *85*(52), 565–569.

Chen, J. M. (1996). Optically-based methods for measuring seasonal variation of leaf area index in boreal conifer stands. *Agricultural and Forest Meteorology*, *80*, 135–163.

Chen, W. J., Black, T. A., Yang, P. C., Barr, A. G., Neumann, H. H., et al. (1999). Effects of climactic variability on the annual carbon sequestration by a boreal aspen forest. *Global Change Biology*, *5*(1), 41–53.

de Beurs, K. M., & Henebry, G. M. (2005). Land surface phenology and temperature variation in the International Geosphere–Biosphere Program high-latitude transects. *Global Change Biology*, *11*, 779–790.

Delbart, N., Kergoat, L., Toan, T., Lhermitte, J., & Picard, G. (2005). Determination of phonological dates in boreal regions using normalized difference water index. *Remote Sensing of Environment*, *97*, 26–38.

Delbart, N., Toan, T., Kergoat, L., & Fedotova, V. (2006). Remote sensing of spring phenology in boreal regions: A free of snow-effect method using NOAA-AVHRR and SPOT-VGT data (1982–2004). *Remote Sensing of Environment*, *101*, 52–62.

Ecological Stratification Working Group (1996). *A National Ecological Framework for Canada*. Ottawa, Ontario, CA: Agriculture and Agri-Food Canada, Research Branch, Centre for Land and Biological Resources Research and Environment Canada, State of Environment Directorate (125pp).

ESRI (2006). Redlands, California, USA.

Gao, B. C. (1996). NDWI—A normalized difference water index for remote sensing of vegetation liquid water from space. *Remote Sensing of Environment*, *58*, 257–266.

Gillett, N. P., Weaver, A. J., Zwiers, F. W., & Flannigan, M. D. (2004). Detecting the effect of climate change on Canadian forest fires. *Geophysical Research Letters*, *31*(18), L18211.

Goetz, S. J., Fiske, G. J., & Bunn, A. G. (2006). Using satellite time-series data sets to analyze fire disturbance and forest recovery across Canada. *Remote Sensing of Environment*, *101*, 352–365.

ITT Visual Information Solutions (2006). Boulder, Colorado, USA.

Johnson, E. A. (1992). *Fire and vegetation dynamics: Studies from the North American boreal forest.* New York: Cambridge Unversity Press.

Fire, climate change and carbon cycling in the boreal forest. Kasischke, E. S., & Stocks, B. J. (Eds.). (2000). *Ecological studies series*, *Vol. 138*. (pp. 274–288)New York: Springer.

Kurz, W. A., & Apps, M. J. (1999). A 70-year retrospective analysis of carbon fluxes in the Canadian forest sector. *Ecological Applications*, *9*, 526–547.

Latifovic, R., & Pouliot, D. (2007). Analysis of climate change impacts on lake ice phenology in Canada using the historical satellite record. *Remote Sensing of Environment*, *106*, 492–507.

Lucht, W., Prentice, I. C., Myneni, R. B., Sitch, S., Friedlingstein, P., et al. (2002). Climactic control of the high-latitude vegetation greening trend and Pinatubo effect. *Science*, *296*, 1687–1689.

Moulin, S., Kergoat, L., Miomy, N., & Dedieu, G. (1997). Global-scale assessment of vegetation phenology using NOAA/AVHRR satellite measurements. *Journal of Climage*, *10*, 1154–1170.

Myneni, R. B., Keeling, C. D., Tucker, C. J., Asrar, G., & Nemani, R. R. (1997). Increased plant growth in the northern latitudes from 1981–1991. *Nature*, *386*, 698–702.

Natural Resources Canada (2006a). *The Atlas of Canada*. Ottawa, Ontario, CA: Natural Resources Canada. Available online at: http://atlas.nrcan.gc.ca/site/english/learningresources/theme_modules/borealforest/index.html

Natural Resources Canada (2006b). *The National Atlas of Canada*. (5th ed., 1978–1995). Ottawa, Ontario, CA: Natural Resources Canada. Available online at: http://atlas.nrcan.gc.ca/site/english/maps/archives/5thedition/environment/ecology/mcr4113

Palko, S., Lowe, J. J., & Pokrant, H. T. (1993). Canada's new seamless forest cover data base. *Proceedings, GIS'93 symposium, Vancouver, CA, February 1993*.

Pisek, J., & Chen, J. M. (2007). Comparison and validation of MODIS and VEGETATION global LAI products over four BigFoot sites in North America. *Remote Sensing of Environment*, *109*, 81–94.

SAS Institute Inc. (2006). Cary, South Carolina, USA.

Schwartz, M. D., Ahas, R., & Aasa, A. (2006). Onset of spring starting earlier across the Northern Hemisphere. *Global Change Biology*, *12*, 343–351.

Serbin, S.P., Gower, S.T., & Ahl, D.E. (submitted for publication). Canopy dynamics and phenology of a boreal black spruce wildfire chronosequence. Agricultural and Forest Meteorology.

Shabanov, N. V., Zhou, L., Knyazikhin, Y., Myneni, R. B., & Tucker, C. J. (2002). Analysis of interannual changes in northern vegetation activity observed in AVHRR data from 1981 to 1994. *IEEE Transactions on Geoscience and Remote Sensing*, *40*(1), 115–130.

Slayback, D. A., Pinzon, J. E., Los, S. O., & Tucker, C. J. (2003). Northern hemisphere photosynthetic trends 1982–99. *Global Change Biology*, *9*, 1–15.

Solomon, S., Qin, D., Manning, M., Alley, R. B., Berntsen, T., et al. (2007). Technical summary. In S. Solomon, D. Qin, M. Manning, Z. Chen, M. Marquis, K. B. Averyt, M. Tignor, & H. L. Miller (Eds.), *Climate change 2007: The physical science basis. Contribution of working group I to the fourth assessment report of the Intergovernmental Panel on Climate Change* New York: Cambridge University Press.

Stocks, B. J. (1991). The extent and impact of forest fires in northern circumpolar countries. In J. Levine (Ed.), *Global biomass burning* (pp. 197–203). Cambridge, MA: MIT Press.

Stocks, B. J., Mason, J. A., Todd, J. B., et al. (2003). Large forest fires in Canada, 1959–1997. *Journal of Geophysical Research — Atmospheres*, *108*(D1), 8149 (2003).

Strong, W. L., Oswald, E. T., & Downing, D. J. (1990). *The Canadian vegetation classification system: First approximation.* Victoria, B.C., Canada: Canadian Forest Service.

Tucker, C. J. (1979). Red and photographic infrared combinations for monitoring vegetation. *Remote Sensing of Environment,*, *8*, 127–150.

Tucker, C. J., Pinzon, J. E., Brown, M. E., Slayback, D., Pak, E. W., Mahoney, R., et al. (2005). An extended AVHRR 8-km NDVI data set compatible with MODIS and SPOT vegetation NDVI data. *International Journal of Remote Sensing*, *26*(20), 4485–4498.

Tucker, C. J., Slayback, D. A., Pinzon, J. E., Los, S. O., Myneni, R. B., & Taylor, M. G. (2001). Higher northern latitude normalized difference vegetation index and growing season trends from 1982–1999. *International Journal of Biometerology,*, *45*, 184–190.

Vermote, E. F., ElSaleous, N., Justice, C. O., et al. (1997). Atmospheric correction of visible to middle-infrared EOS-MODIS data over land surfaces: Background, operational algorithm and validation. *Journal of Geophysical Research — Atmospheres*, *102*(D14), 17131–17141.

Wang, C. K., Bond-Lamberty, B., & Gower, S. T. (2003). Carbon distribution in a well- and poorly-drained black spruce fire chronosequence. *Global Change Biology*(7), 1066–1079.

Zhou, L. M., Tucker, C. J., Kaufmann, R. K., Slayback, D., Shabanov, N. V., & Myneni, R. B. (2001). Variations in northern vegetation activity inferred from satellite data of vegetation index during 1981–1999. *Journal of Geophysical Research*, *106*, 20,069–20,083.